RESEARCH ARTICLE

Open Access

Acanthopagrus schlegelii FADD and caspase-8 are involved in the regulation of apoptosis and inflammation

2025 Volume 2, Article number: e034

https://doi.org/10.48130/animadv-0025-0031

Received: 24 March 2025

Revised: 23 May 2025

Accepted: 8 July 2025

Published online: 1 December 2025

Jianlong Yang[1], Weishang Kong[1], Chuangchuang Wei[1], Xiaoqing Wang[1], Qian Meng[2], Chaofeng Jia[2], Zhiwei Zhang[2], Jiajia Li[3*] and Qingguo Meng[1*]

[1] Jiangsu Key Laboratory for Aquatic Crustacean Diseases, College of Marine Science and Engineering, Nanjing Normal University, 2 Xuelin Road, Nanjing 210023, China

[2] Marine Fisheries Research Institute of Jiangsu Province, Nantong 226007, China

[3] Freshwater Fisheries Research Institute of Jiangsu Province, Nanjing 210017, China

* Corresponding authors, E-mail: jslijj@163.com; mlzzcld@aliyun.com

Citation: Yang J, Kong W, Wei C, Wang X, Meng Q, et al. 2025. *Acanthopagrus schlegelii* FADD and caspase-8 are involved in the regulation of apoptosis and inflammation. *Animal Advances* 2: e034
https://doi.org/10.48130/animadv-0025-0031

Abstract

Acanthopagrus schlegelii is a farmed fish with significant economic value in China. Fas-associated protein with death domain (FADD) and caspase-8 are related to apoptosis and inflammation; however, the specific functions of FADD and caspase-8 in *A. schlegelii* are still unclear. In this study, the open reading frame (ORF) sequence of *AsFADD* and *Ascaspase-8* was 576 and 1,464 bp, encoded 191 amino acids and 487 amino acids, respectively. *AsFADD* and *Ascaspase-8* were highly transcribed in the gills and brain, respectively. The transcription levels of *AsFADD* and *Ascaspase-8* were upregulated in the gills and kidney after infection with *Vibrio parahaemolyticus*. The overexpression of *AsFADD* and *Ascaspase-8* was successfully transfected in RAW264.7 cells and verified by inverted fluorescence microscopy and Western blotting. The overexpressed *AsFADD* was mainly located in the cytoplasm, and *Ascaspase-8* was mainly located in the nucleus of RAW264.7 cells by confocal microscopy. After the overexpression of *AsFADD*, the apoptosis rate of RAW264.7 cells was significantly increased. The interaction between *AsFADD* and *Ascaspase-8* was proved by co-immunoprecipitation (Co-IP). After the overexpression of *AsFADD* and *Ascaspase-8*, the expression of IκBα was significantly increased and the expression of p65 exhibited a marked reduction. Concurrently, significant alterations were observed in the levels of key pro- and anti-inflammatory cytokines, including Interleukin (IL)-1β, IL-6, IL-10, IL-12, and IL-18, whereas a chemotactic factor (IP10) and tumor necrosis factor alpha (TNF-α) were significantly decreased. In summary, this study elucidated the functional roles of *AsFADD* and *Ascaspase-8*, revealing that *AsFADD* promotes apoptosis while suppressing nuclear factor kappa-light-chain-enhancer of activated B cells (NF-κB) signaling activation and inflammatory cytokine secretion.

Introduction

Acanthopagrus schlegeli is mostly distributed in the western Pacific, including China, South Korea, and Vietnam. Valued for its palatability and nutrient-rich profile, *A. schlegeli* has emerged as a commercially vital species within China's aquaculture. In recent years, *A. schlegeli* aquaculture has been expanding[1], in which a more serious problem is *Vibrio parahaemolyticus*-induced skin ulceration. At the initial stage of infection, a large number of white spots appear on the surface of the fish, and the skin of the fish is largely ulcerated as the infection intensifies until death.

As the most important defense line of organisms, the immune system can recognize exogenous substances such as pathogenic microorganisms and regulate the body's rapid immune response. Fish immunity is mainly divided into cellular immunity and humoral immunity. Among them, apoptosis, a genetically regulated form of controlled cell death that serves as a critical mechanism for preserving cellular homeostasis, belongs to cellular immunity[2]. Two well-established pathways govern this process: the inherent mitochondrial pathway and the external death receptor pathway[3]. The death-inducing signaling complex (DISC), a molecular platform formed by Fas-associated protein with death domain (FADD) and caspase-8, plays a critical role in mediating apoptotic signal transduction. The external death receptor pathway chiefly occurs via the binding of specific death receptors to ligands, which causes the domain of the death receptor to oligomerize. Subsequently, it binds to caspase-8, thereby triggering a series of apoptotic responses[4–8]. FADD, a key apoptosis regulator[9,10], features a modular structure comprising a C-terminal death domain (DD) and an N-terminal death effector domain (DEDs)[11]. In the classical apoptotic pathway, the DD domain of the death receptor (Fas) recognizes and binds the DD domain of FADD, and then the DEDs domain of FADD recruits inactive caspase-8 (pro-caspase-8), which, by digestion, activates caspase-8 (c-caspase-8) to trigger a subsequent caspase cascade and ultimately prompts apoptosis[12,13]. Caspase-8 belongs to the caspase family and is one of the key proteins in apoptosis. It is a downstream protein of FADD in the apoptotic signaling pathway. It has two states: one is unactivated caspase-8 (pro-caspase-8) and the other is cleaved caspase-8 (c-caspase-8)[14].

Inflammation is a cascade amplification caused by the activation of Toll-like receptors on immune effector cells to upregulate the manifestation of pro-inflammatory factors[15]. The level of pro-inflammatory factors shows a significant correlation with the nuclear factor kappa-light-chain-enhancer of activated B cells (NF-κB) signaling pathway[16]. NF-κB is a protein complex that has a very important relationship with immunity, inflammation, cell differentiation, and apoptosis[17]. The NF-κB signaling pathway is activated through classical pathways, nonclassical pathways, and other pathways. Classical pathway activation is the main pathway by which NF-κB is activated to play a role, and p65 and p50 are mainly involved[18]. When cells are in a quiescent state, p65/p50/IκBα forms a complex to inhibit NF-κB's

entry into the nucleus[18,19]. When cells are stimulated by lipopolysaccharide (LPS), interleukins (IL), and tumor necrosis factor alpha (TNF-α) and bond to receptors, IκB kinase (IKK) and phosphorylate IκBα can be activated and then degrade, thereby activating the p65/p50/IκBα complex, and then releasing NF-κB and forming dimers[20–23]. When NF-κB translocates into the nucleus, it again prompts cells to produce inflammatory factors such as TNF-α, IL-2, and IL-6[24,25], and again stimulates the activation of the NF-κB signaling pathway.

Inflammation is an important component of immunity. Most of studies in inflammatory genes are in mammals, and little is known about the function of inflammatory genes in *A. schlegelii*. In the present study, the function of *A. schlegelii* FADD and caspase-8 were investigated including their transcription characteristics, overexpression, interaction, regulating apoptosis and inflammation though quantitative reverse transcription–polymerase chain reaction (qRT-PCR), confocal microscopy, Western blotting, co-immunoprecipitation (Co-IP), and so on.

Materials and methods

Animals and bacteria

Five *A. schlegelii* (65 ± 5 g) were obtained from Jiangsu Institute of Marine Fisheries and temporarily cultured in the laboratory for one week. *V. parahaemolyticus* bacteria were also provided by the Jiangsu Institute of Marine Fisheries and stored at −80 °C. The intestines, kidneys, liver, brain, heart, muscles, gills, and blood cells were collected from three healthy *A. schlegelii*.

cDNA cloning and sequence analysis of *AsFADD* and *Ascaspase-8*

The *AsFADD* and *Ascaspase-8* gene sequence were obtained by transcriptome sequencing of *A. schlegelii*. The gene sequences closely matching *AsFADD* and *Ascaspase-8* were examined via BLAST in the NCBI database (https://blast.ncbi.nlm.nih.gov/Blast.cgi). Protein molecular weight and isoelectric point were predicted via ExPASy (https://web.expasy.org/cgi-bin/compute_pi/). The structural prediction of *AsFADD* and *Ascaspase-8* was completed using SMART (http://smart.embl-heidelberg.de/). Multiple sequence alignments were generated using DNAMAN, and phylogenetic tree construction was carried out in MEGA-X via the proximity method and with 1000 bootstraps.

The transcription of *AsFADD* and *Ascaspase-8*

Total RNA was isolated from various tissues using an RNA isolation kit (BioTeke, China). Reverse transcription into cDNA was performed using a reverse transcription kit (Yeasen, China). The tissue distribution of *AsFADD* and *Ascaspase-8* was detected using the SYBR premix ex Ex Taq™ kit (Yeasen, China) by qRT-PCR. The samples were first denatured for 5 min at 95 °C, then underwent 40 amplification cycles (10 s at 95 °C and 30 s at 60 °C). *GAPDH* served as the internal reference gene. Melting curve analysis of the qRT-PCR products was performed to validate amplification specificity, with triplicate biological and technical replicates incorporated into the experimental design. Supplementary Table S1 lists the primers.

V. parahaemolyticus was cultured overnight at 37 °C. Sixty healthy *A. schlegelii* were randomly divided into two groups. The fish in the experimental group and the control group were intraperitoneally injected with 200 μL of *V. parahaemolyticus* [10^7 colony-forming units (CFU)/mL] and 200 μL of phosphate-buffered saline (PBS), respectively. The kidneys and gills were collected at 6, 12, 24, 48, and 72 h after infection. Total RNA from these tissues was isolated and reverse transcribed into cDNA. The transcription characteristics of *AsFADD* and *Ascaspase-8* in *V. parahaemolyticus* infection were detected using qRT-PCR.

The qRT-PCR results were evaluated using GraphPad Prism 8.0. One-way analysis of variance (ANOVA) was used to assess differences between groups, followed by Tukey's *post hoc* test for further analysis. A *p*-value of less than 0.05 was considered to be the boundary to determine statistical significance.

The overexpression of *AsFADD* and *Ascaspase-8*

The corresponding primers (Supplementary Table S1) were designed from the *AsFADD* and *Ascaspase-8* sequences. The mammalian cell expression vectors pEGFP-N1 and pDsRED-Monomer-N1 were digested using *Xho* I and *Age* I restriction enzymes (Takara, Japan) at 37 °C for 20 min. Digested plasmids and target gene fragments were ligated to generate the recombinant plasmids pEGFP–FADD, pEGFP–caspase-8 and pDsRED–caspase-8 using the One Step Cloning Kit (Vazyme, China). RAW264.7 cells were maintained in high-glucose Dulbecco's modified Eagle's medium (DMEM) supplemented with 10% heat-inactivated fetal bovine serum (FBS), 1% penicillin/streptomycin, and cultured under standard conditions (37 °C, 5% CO_2). At 75% confluency, cells were seeded into glass-bottom dishes and transfected with 3 μg recombinant plasmid using Lipofectamine™ 2000 (Thermo, USA). After 24 h, the overexpression efficiency of pEGFP–FADD, pEGFP–caspase-8, and pDsRED–caspase-8 was assessed through fluorescence microscopy (Nikon Ti-E-A1R, Japan) and confirmed via Western blot analysis.

The fluorescence of RAW264.7 cells was observed for 24 h after transfection. After fluorescence was observed, the cells were centrifuged for 5 min (8,000 rpm) to collect the cell. After washing three times with PBS, 400 μL NP-40 lysate and 5 μL phenylmethylsulfonyl fluoride (PMSF) were added and lysed for 30 min on ice. The proteins were denatured by heating at 100 °C for 10 min. The proteins were transferred to polyvinylidene difluoride (PVDF) membranes, followed by electrophoresis on sodium dodecyl sulfate–polyacrylamide gel electrophoresis (SDS-PAGE) gels. The PVDF membrane was placed in an incubation box with 5% skim milk powder and blocked for 2 h. After washing three times with Tris-buffered saline (TBST), primary anti-green fluorescent protein (GFP) mouse monoclonal antibody (1:2,000, TransGen, China) was added and combined for 12 h at 4 °C. After three TBST washes and being incubated for 2 h at room temperature, the secondary anti-mouse immunoglobin G (IgG) (H+L) (1:500, Transgene, China) was washed three times using TBST. Protein expression was detected by ready-to-use hypersensitive electrochemical (ECL) luminescence solution (Vazyme, China).

Following the transfection of pEGFP–FADD or pEGFP–caspase-8, RAW264.7 cells were plated into 35-mm confocal laser scanning dishes. The cells underwent a series of washes with PBS, each lasting 5 min, before being treated with 4% animal tissue cell fixative (Beyotime, China) and then incubated for 15 min. After another round of PBS washes, 4',6-diamidino-2-phenylindole (DAPI) was introduced, and the cells were allowed to incubate for 10 min. Subsequent PBS washes, each lasting 10 min, were performed before applying an anti-fluorescent quencher. Finally, the cells were examined under a confocal laser scanning microscope (Nikon A1R) to analyze the localization of *AsFADD* and *Ascaspase-8*.

The effect of *AsFADD* on cell apoptosis

After 12 h of incubation post-transfection with pEGFP–FADD, the RAW264.7 cells were harvested. Apoptosis was detected by apoptosis detection kit (Beyotime, China) and flow cytometry (FACSverse, BD, USA). Cells were resuspended in 195 μL binding solution, stained with 5 μL Annexin V-PE, and incubated at room temperature in the dark for 15 min. Fluorescence microscopy and flow cytometric analysis (post-resuspension in 800 μL PBS) were performed to quantify apoptotic cells.

Co-immunoprecipitation

Co-IP assays were performed to confirm the interaction between FADD and caspase-8 in RAW264.7 cells. The plasmid pEGFP–FADD and pDsRED–caspase-8 were co-transfected into RAW264.7 cells. After 12 h,

400 μL of NP-40 lysate (Boster, China) and 5 μL of PMSF (Transgen, China) were included and lysed for 30 min on ice. The cell lysates were collected by vortexing them for 10 min (1,400 × *g*) at 4 °C. They were then left to incubate overnight at the same temperature with two specific antibodies: an anti-GFP mouse monoclonal antibody from Transgen in China and a caspase-8 antibody from Abmart, China. Following this, Protein A/G Resin (Transgen, China) was introduced and allowed to incubate at 4 °C for 4 h. After another round of centrifugation at 1,000 ×*g* for 5 min and a thorough rinse with ice-cold PBS three times, the resulting precipitate was analyzed using Western blot techniques.

The effect of *AsFADD* and *Ascaspase-8* on the NF-κB signaling pathway

After transfection with pEGFP–FADD and pEGFP–caspase-8 and incubation for 12 h, the RAW264.7 cells were collected. The protein expression of IκBα and NF-κB p65 were verified using IκBα polyclonal antibody and NF-κB p65 recombinant antibody, respectively (Proteintech, China) by Western blotting. The mRNA transcription of NF-κB was detected by qRT-PCR. Total RNA was extracted from RAW264.7 cells using an extraction kit (BioTeke, China). The primers are listed in Supplementary Table S1.

The effect of *AsFADD* and *Ascaspase-8* on inflammatory factors

RAW264.7 cells were transfected with pEGFP–FADD and pEGFP–caspase-8 and incubated for 6 h. Then heat-inactivated *V. parahaemolyticus* was added to the cells. After another 12 h of culture, the RAW264.7 cells were collected to extracted the total RNA using a total RNA extraction kit (BioTeke, China). The mRNA expression levels were standardized against *GAPDH*, with all experiments conducted in three replicates. Changes in relative gene expression were determined using the $2^{-\Delta\Delta Ct}$ approach. Supplementary Table S1 lists the primers.

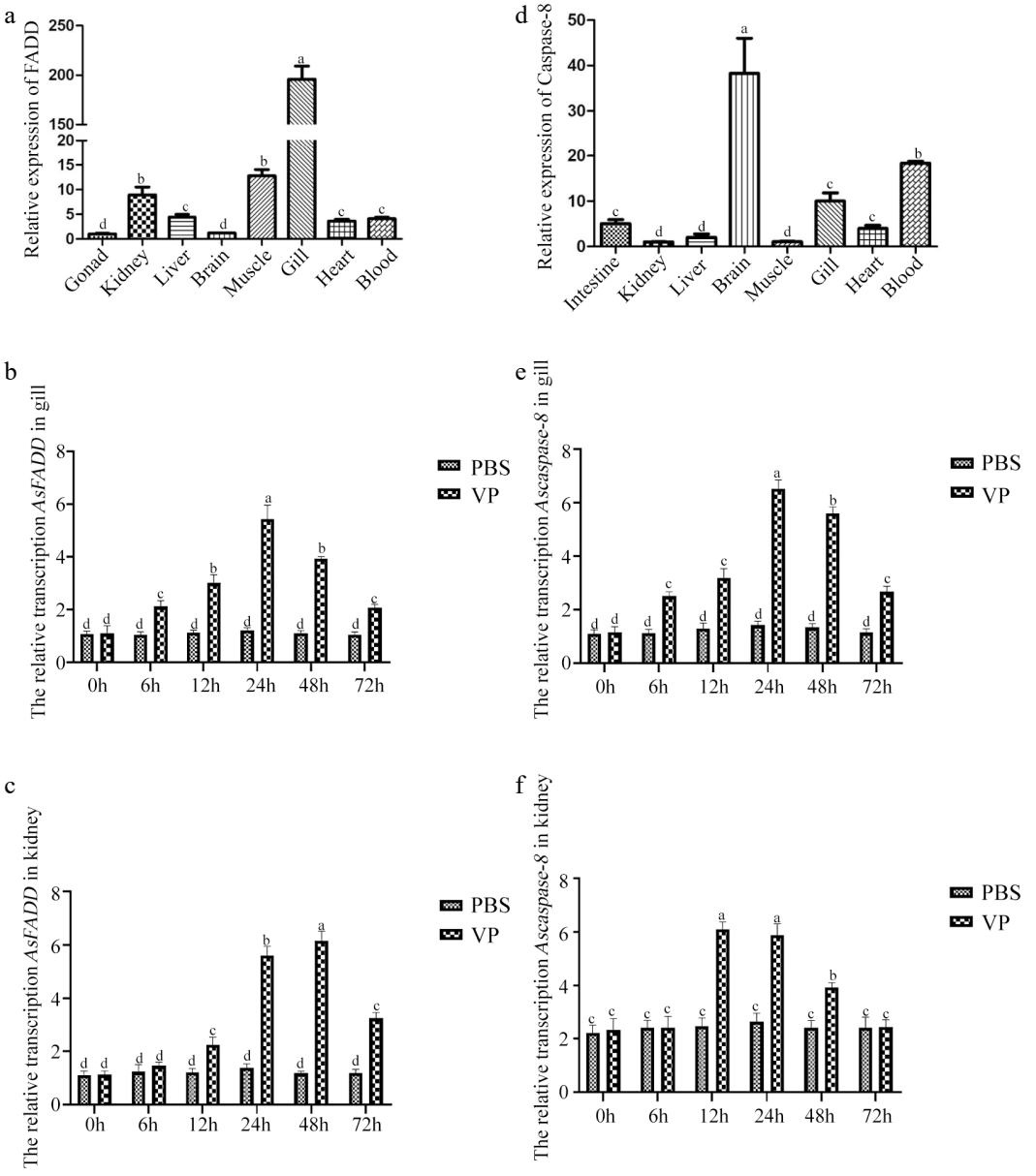

Fig. 1 Distribution of genes in various tissues of *A schlegelii* and the transcription characteristics of genes in the gills and kidneys of *A. schlegelii* after *V. parahaemolyticus* infection. (a) Distribution of *AsFADD* in various tissues. The transcription characteristics of *AsFADD* in the gills (b) and kidneys (c) after *V. parahaemolyticus* infection. (d) Distribution of *Ascaspase-8* in various tissues. The transcription characteristics of *Ascaspase-8* in the gills (e) and kidneys (f) after *V. parahaemolyticus* infection. Error bars represent standard deviations (SD). Different letters on the bars represent statistically significant differences at $p < 0.05$.

Results

Sequence analysis of *AsFADD* and *Ascaspase-8*

The open reading frame (ORF) sequence of *AsFADD* was 576 bp and encoded 191 amino acids. The molecular weight and isoelectric point of *AsFADD* were 21.638 kDa and 5.18, respectively. The protein sequence similarity of FADD between *A. schlegelii* and *Epinephelus lanceolatus*, *Morone saxatilis*, and *Mus musculus* was 63.45%, 61.34%, and 31.33%, respectively. The FADD phylogenetic tree showed that *A. schlegelii* was most closely related to *Sparus aurata*, with 97.22% homology (Supplementary Fig. S1).

The ORF sequence of *Ascaspase-8* spans 1,464 bp, encoding 487 amino acids, with a molecular weight of 54.933 kDa and an isoelectric point of 4.97. The protein sequence similarity of caspase-8 between *A. schlegelii* and *Gasterosteus aculeatus*, *Larimichthys crocea*, and *Lateolabrax maculatus* was 61.84%, 64.08%, and 68.21%, respectively. The caspase-8 phylogenetic tree showed that *Ascaspase-8* was most closely related to *Sparus aurata* (Supplementary Fig. S2).

The transcription characteristics of *AsFADD* and *Ascaspase-8*

The qRT-PCR was used to detect the distribution of *AsFADD* and *Ascaspase-8* in various tissues of healthy *A. schlegelii*. The qRT-PCR showed that *AsFADD* was transcribed ($p < 0.05$) mainly in the gills (Fig. 1a), followed by the muscles and kidneys, but was less transcribed in the gonads and brain. *Ascaspase-8* was transcribed ($p < 0.05$) mainly in the brain, followed by the blood and gills, but was less transcribed in the kidneys and muscles (Fig. 1d). The gills and kidneys of fish can promote immunoactive substances, phagocytose, and remove many bacteria and harmful substances. Therefore, transcriptional changes in *AsFADD* and *Ascaspase-8* in the gills and kidneys following *V. parahaemolyticus* infection were examined by qRT-PCR. The results showed that the transcription of *Ascaspase-8* and *AsFADD* in the gills and kidneys was significantly higher ($p < 0.05$) than that in the PBS group. After *V. parahaemolyticus* infection, the transcription level of *AsFADD* was not significantly different at 0 h, but reached the highest ($p < 0.05$) level at 24 and 48 h in the gills and kidneys, respectively (Fig. 1b, c). The highest transcription ($p < 0.05$) level of *Ascaspase-8* was observed at 24 and 12 h in the gills and kidneys, respectively, but there was no significant difference at 0 h (Fig. 1e, f).

Over-expression of *AsFADD* and *Ascaspase-8* in RAW264.7 cells

The pEGFP–FADD and pEGFP–caspase-8 constructs were generated and introduced into RAW264.7 cells, the transfected cells showed significant green fluorescence under an inverted fluorescence microscope (Fig. 2a). As verified by Western blot analysis, the recombinant protein molecular weight of pEGFP–FADD and pEGFP–caspase-8 were about 50 kDa and 80 kDa, respectively (Fig. 2b). The results demonstrate that the pEGFP–FADD and pEGFP–caspase-8 recombinant plasmids were successfully expressed in RAW264.7 cells. Then the cellular locations of pEGFP–FADD and pEGFP–caspase-8 were investigated. Confocal microscopy revealed *AsFADD* predominantly in the cytoplasm and *Ascaspase-8* primarily in the nucleus (Fig. 2c).

Overexpression of *AsFADD* promotes apoptosis

To verify the apoptosis effect of the overexpression of *AsFADD*, pEGFP-N1 and pEGFP–FADD plasmids were transfected into RAW264.7 cells, and the cells were collected for Western blot, flow cytometry, and

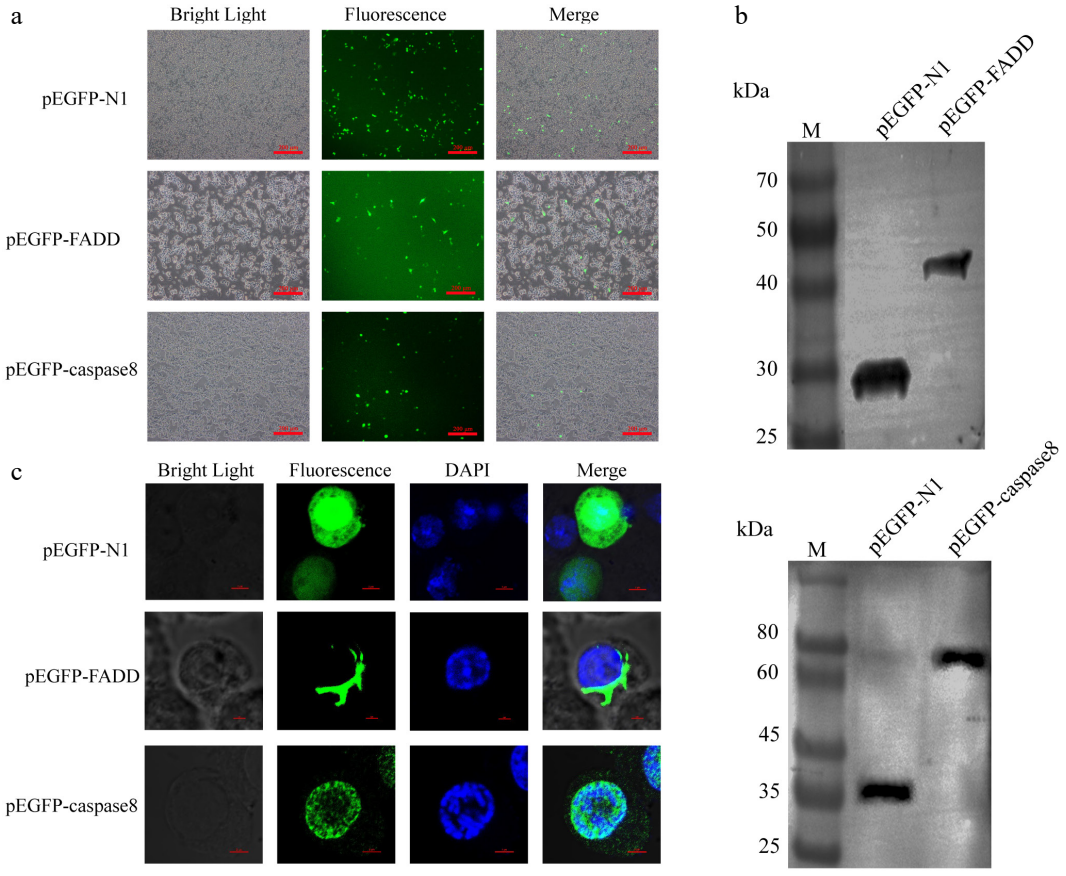

Fig. 2 Overexpression of *AsFADD* and *Ascaspase-8* in RAW264.7 cells. (a) Fluorescence images of expression of the recombinant plasmids pEGFP–FADD and pEGFP–caspase-8, Scale bar, 200 μm. (b) Western blot analysis of pEGFP–FADD and pEGFP–caspase-8. (c) Subcellular localization of pEGFP–FADD and pEGFP–caspase-8 in RAW264.7 cells. Scale bar, 4 μm.

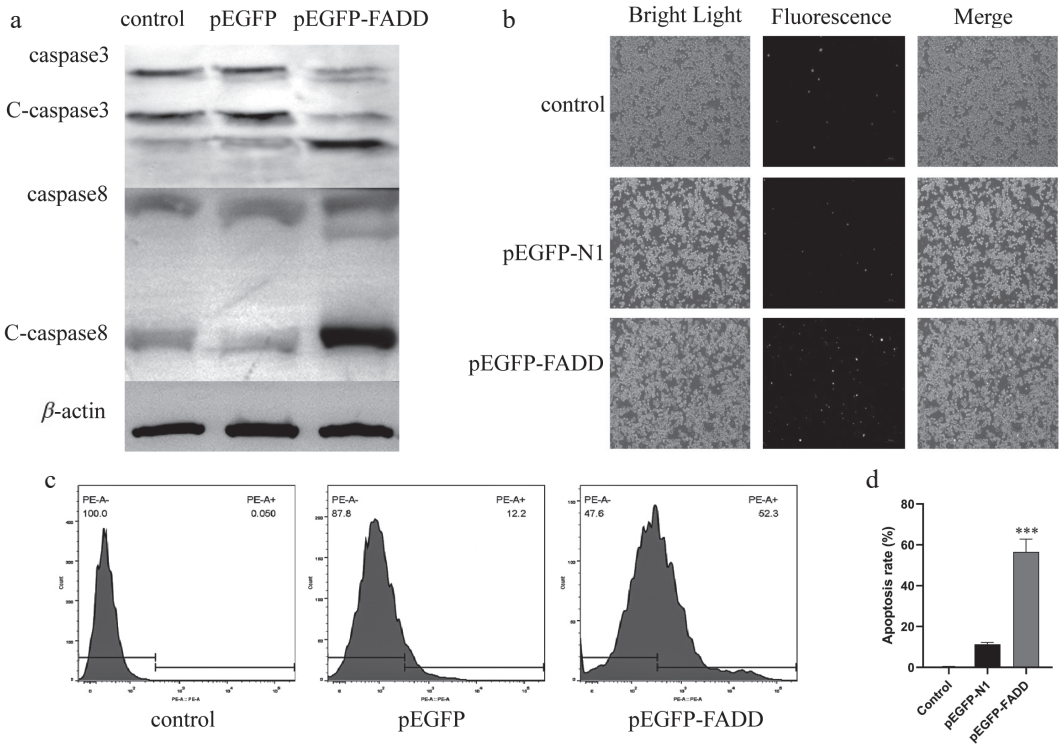

Fig. 3 Effect of overexpression of pEGFP–FADD on apoptosis in RAW264.7 cells. (a) The protein expression levels of c-caspase-3 and c-caspase-8 were detected by Western blot analysis. (b) Apoptosis fluorescence was detected by an inverted fluorescence microscope. Scale bar, 4 μm. (c, d) The percentage of PE-positive cells after pEGFP–FADD overexpression was analyzed by flow cytometry.

fluorescence microscopy analyses. Here, Western blot analysis revealed the elevated expression of cleaved caspase-3 (c-caspase-3) and cleaved caspase-8 (c-caspase-8) in pEGFP–FADD-transfected cells compared with the control and pEGFP-N1 groups (Fig. 3a). Immunofluorescence results verified that the overexpression of *AsFADD* could promote the apoptosis of RAW264.7 cells compared with the control group and pEGFP-N1 group (Fig. 3b). Consistently, fluorescence-activated cell sorting (FACS) analysis demonstrated an increase in phycoerythrin (PE)-positive cells in the *AsFADD* group compared with both the control and pEGFP-N1 cohorts (Fig. 3c, d).

The interactions between *AsFADD* and *Ascaspase-8*

To explore whether FADD and caspase-8 could interact, the pEGFP–FADD and pDsRED–caspase-8 were co-transfected into RAW264.7 cells, and the proteins were purified with anti-GFP antibody. Western blot analysis demonstrated an interaction between EGFP–FADD and DsRED–caspase-8. *AsFADD* was immunoprecipitated with *Ascaspase-8* and vice versa. The results show that *AsFADD* and *Ascaspase-8* could interact intracellularly (Fig. 4a, b).

Apoptosis inhibits the NF-κB signaling pathway and the release of inflammatory factors

To investigate the relationship between apoptosis and the inflammatory response, the NF-κB signaling pathway was detected by Western blotting and qRT-PCR after overexpression of *AsFADD* and *Ascaspase-8* in RAW264.7 cells. The Western blot analysis results showed that the expression of IκBα after transfection with pEGFP–FADD (Fig. 5a, c) or pEGFP–caspase-8 (Fig. 5b, d) were significantly increased, while the expression of p65 protein in the experimental group was significantly decreased. The qRT-PCR analysis further confirmed suppression of the NF-κB pathway in RAW264.7 cells transfected with pEGFP–FADD or pEGFP–caspase-8, characterized by upregulated IκBα transcription and downregulated p65 expression (Fig. 5e, f).

After overexpression of *AsFADD* and *Ascaspase-8* in RAW264.7 cells, the transcription of inflammatory factors was quantified. The findings indicated that when infected with *V. parahaemolyticus*, the expression levels of interleukin (IL-1β, IL-6, IL-10, IL-12, IL-18) and a chemokine (IP10) were also notably diminished in comparison with pEGFP-N1. These results demonstrated that the production and release of inflammation factors in the cells were inhibited when apoptosis was activated (Fig. 6a, b).

Discussion

FADD, a pivotal adaptor protein, facilitates apoptotic signaling cascades initiated by death receptors (DRs)[26]. Moreover, caspase-8 is one of the key proteins downstream of FADD in the apoptosis signaling pathway and plays a vital role in immunity-related processes together with FADD[27]. In this study, *A. schlegelii* FADD and caspase-8 were cloned and characterized. RT-qPCR showed that they were distributed in all tissues examined. The expression levels of FADD and caspase-8 in the heart and liver of *A. schlegelii* were upregulated after stimulation with *V. parahaemolyticus*, which had positive immunoregulatory effects. In hybrid yellow catfish, FADD mediated immune responses to *Aeromonas hydrophila* and *Edwardsiella tarda* infections[28]. The distribution of FADD was highest in the liver, gills, muscle, head, and kidney of grouper, and FADD transcription in the liver was significantly increased after stimulated by Singapore grouper iridovirus (SGIV) and polyinosinic: polycytidylic acid [Poly(I:C)][29]. After stimulation, the expression and phosphorylation of *Paralichthys olivaceus* FADD in immune-related tissues were increased[30]. The mRNA levels of FADD, caspase-3, and caspase-8 in carp tissues were increased when stimulated by a virus[31]. FADD is a key mediator of the Toll-like receptor (TLR)-independent cytosolic double-stranded (ds)RNA-sensing pathway and a component of the innate immune signaling pathway in immune deficiency (IMD) in *Drosophila*[32]. Caspase-8 was mainly distributed in the liver, spleen, and gills of large yellow crocea, with a low distribution in the brain[33]. Similarly, in *Trachinotus ovatus*, caspase-8 and caspase-8-like genes were significantly upregulated at transcriptional levels after LPS and Poly(I:C)

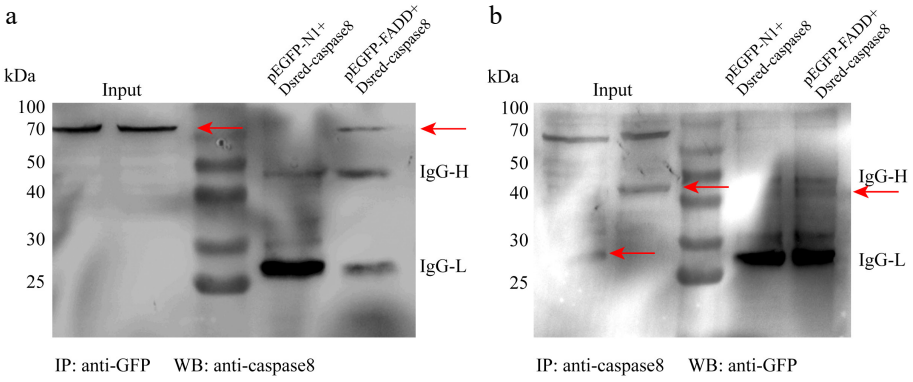

Fig. 4 The interaction between FADD and caspase-8. Raw264.7 cells were transfected with pEGFP-N1 or pEGFP–FADD and DsRED–caspase-8 for 48 h. Co-IP assays were performed using anti-GFP (a) and anti-caspase-8 (b).

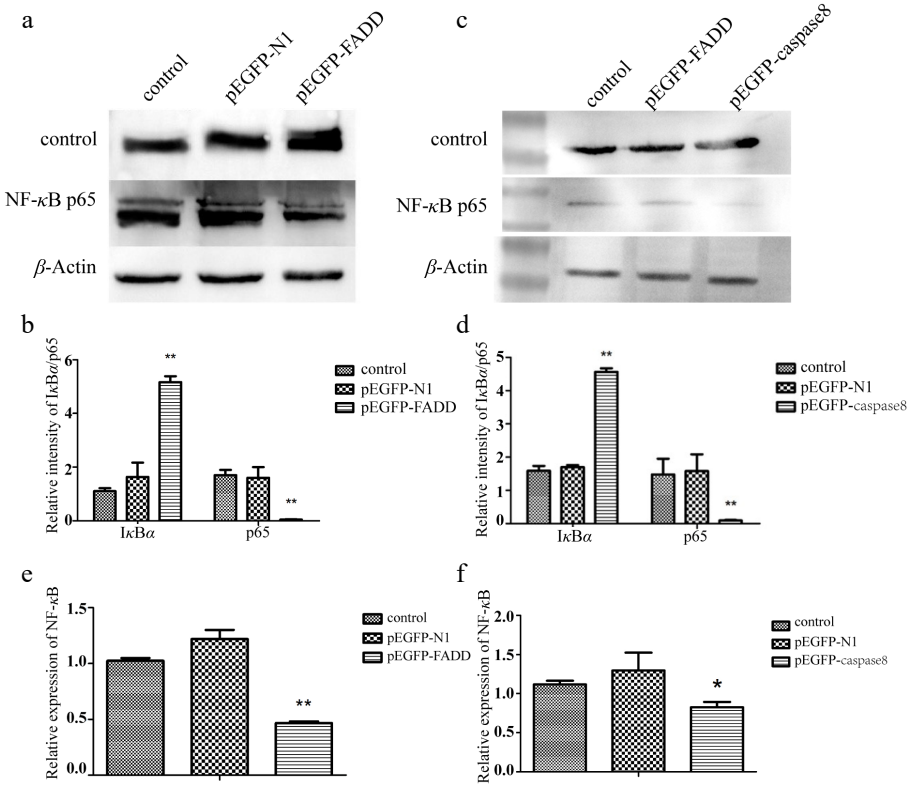

Fig. 5 Effect of the overexpression of pEGFP–FADD and pEGFP–caspase-8 on the NF-κB signaling pathway detected by Western blotting. (a, c) The expression levels of IκBα and p65 were detected by Western blotting. (b, d) The gray value of the strip was quantitatively analyzed with *GAPDH* as the internal parameter. (e) Effect of the overexpression of pEGFP–FADD on NF-κB transcription detected by qRT-PCR. (f) Effect of the overexpression of pEGFP–caspase-8 on NF-κB transcription levels detected by qRT-PCR, using GAPDH as an endogenous control. Vertical bars represent the mean ± standard error (SE) ($n = 3$), and significant differences are marked with asterisks (* $p < 0.05$, ** $p < 0.01$).

stimulation[34]. Together, these findings highlight the conserved involvement of FADD and caspase-8 in innate immune defense.

The subcellular location of FADD was in the cytoplasm, showing that FADD is a cytosolic protein[35,36]. Whereas pro-caspase-8 was also predominantly cytoplasm, a small amount is expressed in the nucleus[37]. During apoptosis, nuclear envelope disintegration facilitates the proteolytic activation of pro-caspase-8 into c-caspase-8, which subsequently accumulates at perinuclear regions. Subcellular fractionation analyses in this study further revealed distinct compartmentalization patterns, as *AsFADD* was predominantly localized in the cytoplasm, while *Ascaspase-8* was mainly concentrated in the nucleus. To further explore the functional role of FADD and caspase-8 in apoptosis, the recombinant plasmids pEGFP-N1–FADD and pEGFP-N1–caspase-8 were constructed using *A. schlegelii* FADD and caspase-8, and co-transfected into mouse macrophages. Co-IP analysis verified that FADD and caspase-8 could interact to form a signal inducer. Apoptosis, an evolutionarily conserved and genetically orchestrated form of programmed cell death, is activated by diverse physiological or pathological stimuli. It is also an important biological process and plays an important role in cellular immunity[38]. Accumulating evidence highlights FADD and caspase-8 as pivotal regulators of apoptotic signaling. For example, overexpression of FADD triggers apoptotic pathways independently of FAS ligand engagement and drives caspase-3's activation in B16F10 melanoma models[39,40]. Moreover, FADD triggered apoptosis in both primary murine tubular epithelium cultures and the murine cortical tubular cell line[41]. After *Amphioxus baicalensis* FADD was transfected into Hela cells, the FADD could induce apoptosis of cancer cells and resist cancer[42]. In

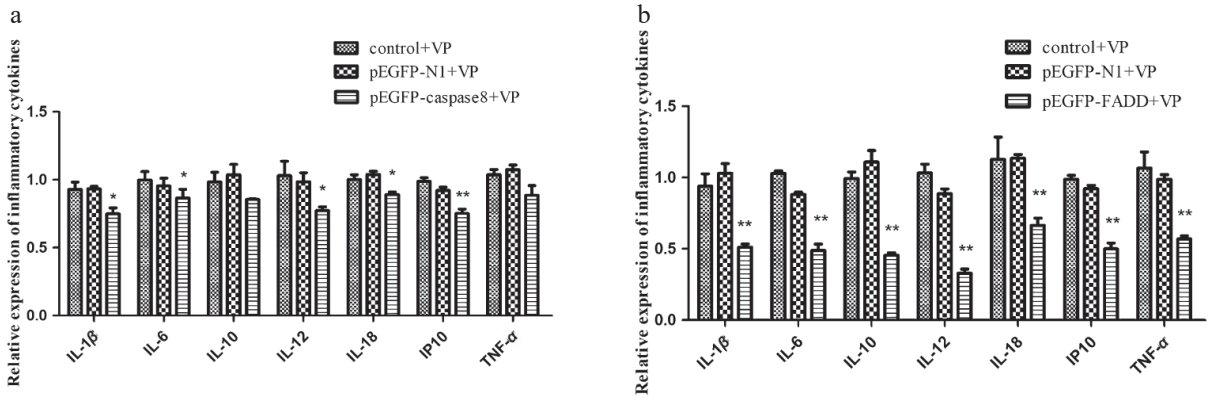

Fig. 6 The effect of the overexpression of pEGFP–caspase-8 on downstream inflammatory factors when infected with *V. parahaemolyticus*. The expression levels of IL-1*β*, IL-6, IL-10, IL-12, IL-18, IP10, and TNF-*α* were detected by qRT-PCR, and GAPDH was used as internal reference. (a) pEGFP–FADD. (b) pEGFP–caspase-8. Vertical bars represent the mean ± SE (n = 3), and significant differences are marked with asterisks (* $p < 0.05$, ** $p < 0.01$).

the present study, the overexpression of *AsFADD* could also promote apoptosis. DISC is involved in apoptosis signal transduction and is a complex composed of FADD and caspase-8. Human FADD may interact with pro-caspase-8 in cancer cells, whereas the association of the anti-apoptotic protein cFLIPL with DISC is diminished[11]. Additionally, TRAIL's (TNF-related apoptosis-inducing ligand, TRAIL) interaction with DR4/DR5 death receptors induces the formation of the DISC, where FADD acts as a molecular adaptor to orchestrate recruitment of caspase-8[43]. Structural studies further revealed that FADD's DD facilitates its interaction with procaspase-8, mirroring the binding mechanism observed between FADD and Fas DD[44]. In the present study, it was verified that *AsFADD* and *Ascaspase-8* could interact with each other. Therefore, we speculate that *AsFADD* and *Ascaspase-8* are involved in the cellular immune response mechanism by interacting to form the DISC, which activated apoptosis.

To further explore the effect of apoptosis on cellular inflammation, Western blotting and RT-PCR were used to detect the changes in *A. schlegelii* apoptosis-related proteins after FADD and caspase-8 were overexpressed in the macrophages. Related studies have shown that FADD and caspase-8 not only play a key role in apoptosis but are also associated with the NF-*κ*B signaling pathway and inflammation. After human FADD was overexpressed in MCF7 and HCT116 cancer cells, the expression levels of IKK, p65 and p-p65 decreased, while the expression levels of I*κ*B*α* increased[11], indicating that mammalian apoptotic proteins could inhibit NF-*κ*B activity. In this study, after the apoptosis-related proteins *AsFADD* and *Ascaspase-8* were overexpressed in RAW264.7 cells, the NF-*κ*B signaling pathway was inhibited, which was the same as the inhibitory trend in mammalian cells[45]. LPS could activate the NF-*κ*B pathway and promote IL-6 secretion, but both NF-*κ*B and IL-6 were inhibited in FADD-null mouse fibroblasts[46]. Similarly, knockdown of caspase-8 revealed the inhibition of both IL-1*β* and IL-18[47,48]. In the present study, *AsFADD* and *Ascaspase-8* could inhibit the transcription of inflammatory factors. Therefore, apoptosis could negatively regulate the inflammatory response when it is activated.

Conclusions

In this study, the qRT-PCR results showed that the transcriptional levels of *AsFADD* and *Ascaspase-8* in the gills and kidneys were significantly changed after *V. parahaemolyticus* infection. Confocal laser scanning microscopy showed that *AsFADD* and *Ascaspase-8* were mainly located in the cytoplasm and nucleus, respectively. When *AsFADD* was overexpressed in RAW264.7 cells, cell apoptosis was activated. Co-IP analysis revealed there was an interaction between FADD and caspase-8. These results suggested that *AsFADD* and *Ascaspase-8* are involved in apoptosis. Western blotting and qRT-PCR showed that the overxpression of *AsFADD* inhibited the NF-*κ*B signaling pathway and the transcription of interleukins (IL-1*β*, IL-6, IL-10, IL-12, IL-18), IP10, and TNF-*α* in *V. parahaemolyticus* infection. Overexpression of *Ascaspase-8* had no significant effect on IL-10 and TNF-*α*, but had the effect on the other interleukins and IP10. These results indicate that when apoptosis was activated, the production and release of inflammation-related factors were inhibited. This study provides a theoretical basis for further research into disease resistance and breeding of *A. schlegelii*.

Ethical statements

All procedures were reviewed and preapproved by the Institutional Animal Care and Use Committee of Nanjing Normal University (identification number: IACUC-2025082, approval date: 2025-02-16) and performed in accordance with the Guide for the Care and Use of Laboratory Animals of the National Institutes of Health. The research followed the 'Replacement, Reduction, and Refinement' principles to minimize harm to animals. This article provides details on the housing conditions, care, and pain management for the animals, ensuring that the impact on the animals was minimized during the experiment.

Author contributions

The authors confirm their contributions to the paper as follows: methodology, investigation, and writing – original draft: Yang J, Kong W; validation, resources, and data curation: Wei C, Wang X, Meng Q, Jia C, Zhang Z; supervision and writing – review and editing: Li J, Meng Q. All authors reviewed the results and approved the final version of the manuscript.

Data availability

The datasets generated and analyzed during the current study are available from the corresponding author on reasonable request.

Acknowledgments

The current work was supported by grants from the Genetic Improvement of Sea Bream and Creation of New Strains (Grant No. PZCZ201744), Jiangsu Provincial Agricultural Project (Grant No. 2023-SJ-030), Major Agricultural Technology Collaborative Promotion Project (Grant No. 2021-ZYXT-09), and the Postgraduate Research & Practice Innovation Program of Jiangsu Province (2024).

Conflict of interest

The authors declare that they have no conflict of interest.

Supplementary information accompanies this paper at (https://www.maxapress.com/article/doi/10.48130/animadv-0025-0031)

References

1. Xiang XW, Xiao JX, Zhou YF, Zheng B, Wen ZS. 2019. Liver transcriptome analysis of the *Sparus macrocephlus* in response to *Vibrio parahaemolyticus* infection. *Fish & Shellfish Immunology* 84:825–33
2. Adams JM. 2003. Ways of dying: multiple pathways to apoptosis. *Genes & Development* 17(20):2481–95
3. Li H, Zhu H, Xu CJ, Yuan J. 1998. Cleavage of BID by caspase-8 mediates the mitochondria damage in the Fas pathway of apoptosis. *Cell* 94(4):491–501
4. Wiley SR, Schooley K, Smolak PJ, Din WS, Huang CP, et al. 1995. Identification and characterization of a new member of the TNF family that induces apoptosis. *Immunity* 3(6):673–82
5. Guicciardi ME, Gores GJ. 2009. Life and death by death receptors. *The FASEB Journal* 23(6):1625–37
6. Ashkenazi A, Salvesen G. 2014. Regulated cell death: signaling and mechanisms. *Annual Review of Cell and Developmental Biology* 30:337–56
7. von Karstedt S, Montinaro A, Walczak H . 2017. Exploring the TRAILs less travelled: TRAIL in cancer biology and therapy. *Nature Reviews Cancer* 17(6):352–66
8. Lossi L. 2022. The concept of intrinsic versus extrinsic apoptosis. *Biochemical Journal* 479(3):357–84
9. Gulbins E, Jekle A, Ferlinz K, Grassmé H, Lang F. 2000. Physiology of apoptosis. *American Journal of Physiology-Renal Physiology* 279(4): F605–F615
10. Reece SE, Pollitt LC, Colegrave N, Gardner A. 2011. The meaning of death: evolution and ecology of apoptosis in protozoan parasites. *PLoS Pathogens* 7(12):e1002320
11. Ranjan K, Waghela BN, Vaidya FU, Pathak C. 2020. Cell-penetrable peptide-conjugated FADD induces apoptosis and regulates inflammatory signaling in cancer cells. *International Journal of Molecular Sciences* 21(18):6890
12. Oppenheim RW, Flavell RA, Vinsant S, Prevette D, Kuan CY, et al. 2001. Programmed cell death of developing mammalian neurons after genetic deletion of caspases. *The Journal of Neuroscience* 21(13):4752–60
13. Peña-Blanco A, García-Sáez AJ. 2018. Bax, Bak and beyond—mitochondrial performance in apoptosis. *The FEBS Journal* 285(3):416–31
14. Mnich K, Koryga I, Pakos-Zebrucka K, Thomas M, Logue SE, et al. 2021. The stressosome, a caspase-8-activating signalling complex assembled in response to cell stress in an ATG5-mediated manner. *Journal of Cellular and Molecular Medicine* 25:8809–20
15. Kjell J, Olson L. 2016. Rat models of spinal cord injury: from pathology to potential therapies. *Disease Models & Mechanisms* 9(10):1125–37
16. Saxena T, Loomis KH, Pai SB, Karumbaiah L, Gaupp E, et al. 2015. Nanocarrier-mediated inhibition of macrophage migration inhibitory factor attenuates secondary injury after spinal cord injury. *ACS Nano* 9(2):1492–505
17. Chu Y, Xu Y, Yang W, Chu K, Li S, et al. 2023. N-acetylcysteine protects human periodontal ligament fibroblasts from pyroptosis and osteogenic differentiation dysfunction through the SIRT1/NF-κB/Caspase-1 signaling pathway. *Archives of Oral Biology* 148:105642
18. Ranjan K, Pathak C. 2016. FADD regulates NF-κB activation and promotes ubiquitination of cFLIPL to induce apoptosis. *Scientific Reports* 6:22787
19. Chen L, Zheng L, Chen P, Liang G. 2020. Myeloid differentiation primary response protein 88 (MyD88): the central hub of TLR/IL-1R signaling. *Journal of Medicinal Chemistry* 63(22):13316–29
20. Apriawan T, Widjiati W, Utomo DN, Fauzi AA, Subagio EA, et al. 2022. Periosteum-induced ossification effect in skull defect through interleukin-8 and NF-κB pathway: an experimental study with *Oryctolagus cuniculus* rabbits. *Surgical Neurology International* 13:140
21. Dlouhy I, Armengol M, Recasens-Zorzo C, Ribeiro ML, Pérez-Galán P, et al. 2022. Interleukin-1 receptor-associated kinase 1/4 and bromodomain and extra-terminal inhibitions converge on NF-κB blockade and display synergistic antitumoral activity in activated B-cell subset of diffuse large B-cell lymphoma with *MYD88* L265P mutation. *Haematologica* 107(12):2990
22. Yang S, Sui W, Ren X, Wang X, Bu G, et al. 2023. UNC93B1 facilitates TLR18-mediated NF-κB signal activation in *Schizothorax prenanti*. *Fish & Shellfish Immunology* 134:108584
23. Liu Y, Meng C, Li Y, Xia D, Lu C, et al. 2023. Peptide-protected gold nanoclusters efficiently ameliorate acute contact dermatitis and psoriasis via repressing the TNF-α/NF-κB/IL-17A axis in keratinocytes. *Nanomaterials* 13(4):662
24. Zhao J, He X, Zuo M, Li X, Sun Z. 2021. Anagliptin prevented interleukin 1β (IL-1β)-induced cellular senescence in vascular smooth muscle cells through increasing the expression of sirtuin1 (SIRT1). *Bioengineered* 12(1):3968–77
25. Guo LW, Wang YK, Li SJ, Yin GT, Li D. 2023. Elevated fibroblast growth factor 23 impairs endothelial function through the NF-κB signaling pathway. *Journal of Atherosclerosis and Thrombosis* 30(2):138–49
26. Wallach D, Varfolomeev EE, Malinin NL, Goltsev YV, Kovalenko AV, et al. 1999. Tumor necrosis factor receptor and Fas signaling mechanisms. *Annual Review of Immunology* 17:331–67
27. Kumar S. 2007. Caspase function in programmed cell death. *Cell Death and Differentiation* 14(1):32–43
28. Guo S, Zeng M, Chen L, Chen H, Gao W, et al. 2023. Characterization and expression profiling of fadd gene in response to exogenous *Aeromonas hydrophila* or *Edwardsiella tarda* challenge in the hybrid yellow catfish (*Pelteobagrus fulvidraco* ♀ × *P. vachelli* ♂). *Fish & Shellfish Immunology* 141:109021
29. Zhang X, Zang S, Li C, Wei J, Qin Q. 2018. Molecular cloning and characterization of FADD from the orange-spotted grouper (*Epinephelus coioides*). *Fish & Shellfish Immunology* 74:517–29
30. Kang CW, Kim NH, Park NG, Kim GD. 2016. Apoptotic cell death induced by ofLBP6A, lipopolysaccharide binding protein model peptide, derived from *Paralichthy olivaceus* on MKN-28 cells. *Drug Development Research* 77(2):94–102
31. Zhang H, Zhao F, Gai X, Cai J, Zhang X, et al. 2022. Astilbin attenuates apoptosis induced by cadmium through oxidative stress in carp (*Cyprinus carpio* L.) head kidney lymphocyte. *Fish & Shellfish Immunology* 125:230–37
32. Balachandran S, Thomas E, Barber GN. 2004. A FADD-dependent innate immune mechanism in mammalian cells. *Nature* 432:401–5
33. Yang B, Yin Z, Gao S, Chen M, Xu D, et al. 2021. Characterization of Caspase8 and its role in the regulation of apoptosis-related genes in large yellow croaker (*Larimichthys crocea*). *Aquaculture* 539:736595
34. Da F, Wan XJ, Lin GX, Jian JC, Cai SH. 2022. Cloning, characterization and expression analysis of caspase-8 genes from the golden pompano (*Trachinotus ovatus*). *Frontiers in Marine Science* 9:1093176
35. Yang YW, Zhang CM, Huang XJ, Zhang XX, Zhang LK, et al. 2016. Tumor-targeted delivery of a C-terminally truncated FADD (N-FADD) significantly suppresses the B16F10 melanoma via enhancing apoptosis. *Scientific Reports* 6:34178
36. Gómez-Angelats M, Cidlowski JA. 2003. Molecular evidence for the nuclear localization of FADD. *Cell Death & Differentiation* 10:791–97
37. Sun W, Li H, Hui H. 2022. Research advances of the relationship between caspase-8 in programmed cell death and disease. *Journal of Contemporary Medical Practice* 4(4):112–17
38. Kerr JFR, Wyllie AH, Currie AR. 1972. Apoptosis: a basic biological phenomenon with wideranging implications in tissue kinetics. *British Journal of Cancer* 26(4):239–57
39. Chinnaiyan AM, O'Rourke K, Tewari M, Dixit VM. 1995. FADD, a novel death domain-containing protein, interacts with the death domain of Fas and initiates apoptosis. *Cell* 81(4):505–12

40. Lu Z, Tang M, Li Y, Shi F, Zhan F, et al. 2021. Molecular cloning and characterization of FADD from the grass carp (*Ctenopharyngodon idellus*) in response to bacterial infection. *Aquaculture* 542:736829
41. Justo P, Sanz AB, Lorz C, Egido J, Ortiz A. 2006. Lethal activity of FADD death domain in renal tubular epithelial cells. *Kidney International* 69(12):2205–11
42. Zhang J, Huang B, Gao Q, Nie P. 2009. Cloning and functional study of FADD in *Branchiostoma belcheri*. *Acta Hydrobiologica Sinica* 33(6):1175–84
43. Agata N, Ahmad R, Kawano T, Raina D, Kharbanda S, et al. 2008. MUC1 oncoprotein blocks death receptor-mediated apoptosis by inhibiting recruitment of caspase-8. *Cancer Research* 68(15):6136–44
44. Yan Q, McDonald JM, Zhou T, Song Y. 2013. Structural insight for the roles of fas death domain binding to FADD and oligomerization degree of the Fas-FADD complex in the death-inducing signaling complex formation: a computational study. *Proteins: Structure, Function, and Bioinformatics* 81(3):377–85
45. Hernandez L, Kim MK, Noonan AM, Sagher E, Kohlhammer H, et al. 2015. A dual role for Caspase8 and NF-κB interactions in regulating apoptosis and necroptosis of ovarian cancer, with correlation to patient survival. *Cell Death Discovery* 1(1):15053
46. Bannerman DD, Eiting KT, Winn RK, Harlan JM. 2004. FLICE-like inhibitory protein (FLIP) protects against apoptosis and suppresses NF-κB activation induced by bacterial lipopolysaccharide. *The American Journal of Pathology* 165(4):1423–31
47. Gurung P, Anand PK, Malireddi RK, Vande Walle L, Van Opdenbosch N, et al. 2014. FADD and caspase-8 mediate priming and activation of the canonical and noncanonical Nlrp3 inflammasomes. *Journal of Immunology* 192(4):1835–46
48. Bannerman DD, Tupper JC, Kelly JD, Winn RK, Harlan JM. 2002. The Fas-associated death domain protein suppresses activation of NF-κB by LPS and IL-1β. *Journal of Clinical Investigation* 109:419–25